



Research Article

High throughput determination of infectious virus titers by kinetic measurement of infection-induced changes in cell morphology

Dominik Hotter ¹, Marco Kunzelmann ², Franziska Kiefer ¹, Chiara Leukhardt ¹, Carolin Fackler ¹, Stefan Jäger ³ and Johannes Solzin ¹

¹ Boehringer Ingelheim Pharma GmbH & Co. KG, Viral Therapeutics Center, Birkendorfer Straße 65, 88397 Biberach an der Riß, Germany

² Boehringer Ingelheim Pharma GmbH & Co KG, Development Biologicals, Birkendorfer Straße 65, 88397 Biberach an der Riß, Germany

³ Boehringer Ingelheim Pharma GmbH & Co KG, Central Nervous System Diseases Research, Birkendorfer Straße 65, 88397 Biberach an der Riß, Germany

* Correspondence: johannes.solzin@boehringer-ingelheim.com

Supplements

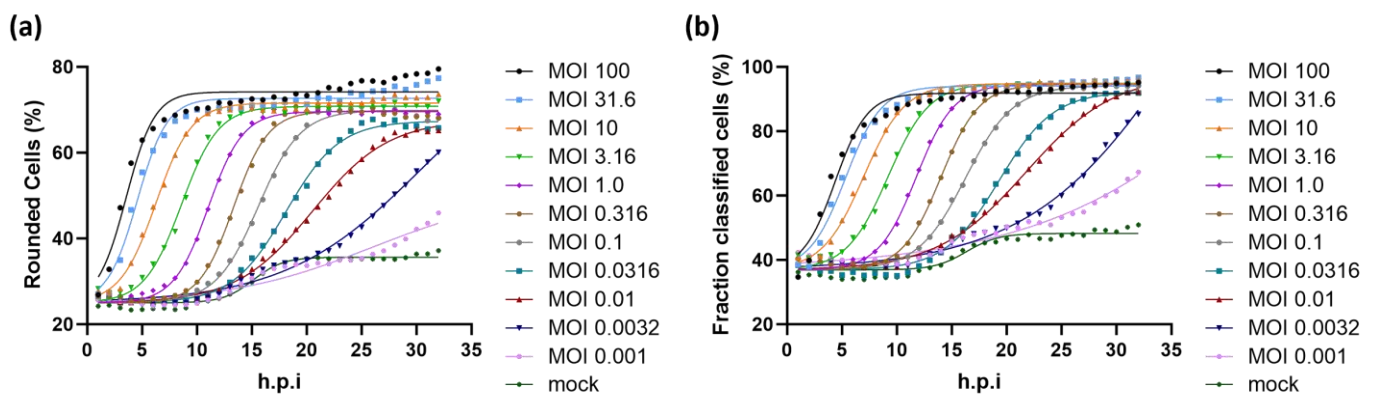
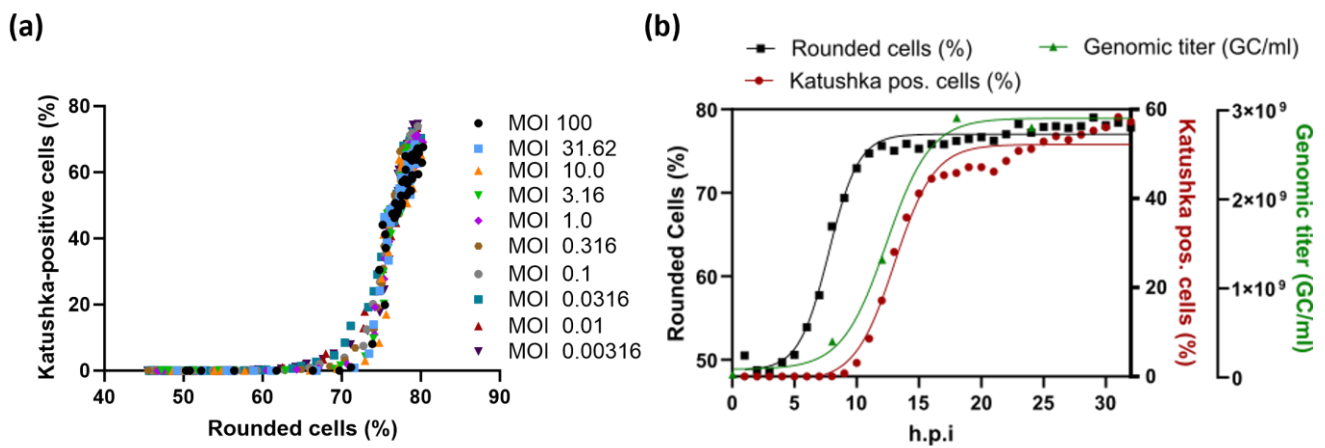


Figure S1. Different algorithms yield similar results for infection-induced cellular changes. BHK-21 cells were infected with VSV-GP at the indicated MOI. Bright field images of the infected cells were acquired in 1 h intervals and analyzed applying different algorithms in Columbus. Each point represents the mean of eight wells. Lines represent the result of a non-linear kinetic fit with global lower asymptote for all curves. (a) The proportion of rounded cells normalized to the total cell number was determined. Cells were defined as rounded if the ratio of their smallest cell diameter to the largest cell diameter exceeds 0.3 (compare to results presented in Figure 1 generated using Gen5). (b) Two cell fractions were discriminated based on a linear classifier, which integrates multiple cellular parameters including roundness, length-width-ratio, area, intensity and surface texture.



25

Figure S2. Temporal relation between cell rounding, viral gene expression and viral replication. (a) BHK-21 cells were infected at the indicated MOI with a VSV-GP variant expressing the red fluorescent Katushka protein. The proportion of rounded cells relative to the total cell number was determined based on bright-field images. In the same field of view, fluorescence was determined with an excitation/emission wavelength of 584±20 nm/625±20 nm. Katushka positive cells are expressed as percentage of the total number of cells in the bright field image. Each point represents the mean of four wells. (b) BHK-21 cells were infected at an MOI of 10 and brightfield and fluorescence images were acquired as described for (a). Rounded cells and Katushka positive cells are both expressed as percentage of the total number of cells in the bright field image. Each point represents the mean of three wells. A second plate was infected and incubated in parallel and used to harvest supernatants at 0, 8, 12, 18 and 24 h.p.i. Genomic virus titers expressed as genomic copies (GC) per ml were determined by qRT-PCR to monitor viral replication. A non-linear 4 parameter logistic model was applied to fit the curve.

26
27
28
29
30
31
32
33
34
35
36
37
38

Table S1. Tabulated results of intra-plate precision of the KIT assay. The KIT assay was used to determine the titer of a sample with an actual titer of 1.39E+09 TCID₅₀/ml. To control assay performance throughout its working range, a sample was tested at three different target MOIs, which was achieved by three different 10-fold pre-dilutions. For each target MOI, six independent measurements were performed (see Figure 4b). Variability is expressed as coefficient of variation (CV).

39
40
41
42
43

| Target MOI | Measured titer (TCID ₅₀ /ml) | Mean titer (TCID ₅₀ /ml) | CV (%) | Overall CV (%) | Overall mean titer (TCID ₅₀ /ml) | Overall mean recovery (%) |
|------------|---|-------------------------------------|--------|----------------|---|---------------------------|
| 17.8 | 1.50E+09 | 1.52E+09 | 4.10 | 10.86 | 1.35E+09 | 97.02 |
| | 1.47E+09 | | | | | |
| | 1.57E+09 | | | | | |
| | 1.53E+09 | | | | | |
| | 1.59E+09 | | | | | |
| | 1.43E+09 | | | | | |
| 1.78 | 1.15E+09 | 1.24E+09 | 5.61 | 10.86 | 1.35E+09 | 97.02 |
| | 1.25E+09 | | | | | |
| | 1.28E+09 | | | | | |
| | 1.25E+09 | | | | | |
| | 1.33E+09 | | | | | |
| | 1.16E+09 | | | | | |
| 0.18 | 1.28E+09 | 1.29E+09 | 8.10 | 10.86 | 1.35E+09 | 97.02 |
| | 1.44E+09 | | | | | |

| | | | | | |
|--|----------|--|--|--|--|
| | 1.40E+09 | | | | |
| | 1.17E+09 | | | | |
| | 1.21E+09 | | | | |
| | 1.26E+09 | | | | |

Table S2. Tabulated results of precision and accuracy of the KIT assay for determination of NDV titers. Time-dependent cell rounding after infection of DF-1 chicken fibroblasts with NDV was determined at different MOIs. RT50 values were calculated and plotted against the corresponding MOI. A sigmoidal four parameter logistic fit was applied to the RT50 values to generate a standard curve, which was used to interpolate MOIs of three samples (M 1-M 3) tested at four different concentrations (see Figure 6b). Recovery of the actual sample titer (3.80E+08 TCID50/ml) and variability expressed as coefficient of variation (CV) are shown.

| Target MOI | Measured titer (TCID50/ml) | | | Mean titer (TCID50/ml) | CV% | Overall mean titer (TCID50/ml) | Overall CV% | Recovery (%) |
|------------|----------------------------|----------|----------|------------------------|-------|--------------------------------|-------------|--------------|
| | M 1 | M 2 | M 3 | | | | | |
| 3.16 | 3.76E+08 | 4.24E+08 | 3.88E+08 | 3.96E+08 | 6.36 | 4.05E+08 | 12.92 | 106.64 |
| 10 | 3.94E+08 | 3.65E+08 | 4.13E+08 | 3.91E+08 | 6.11 | | | |
| 31.6 | 4.97E+08 | 3.90E+08 | 5.11E+08 | 4.66E+08 | 14.22 | | | |
| 100 | 4.10E+08 | 3.38E+08 | 3.56E+08 | 3.68E+08 | 10.27 | | | |

44
45
46
47
48
49
50